PROTEIN FOLDING

Dr. Rita P.-Y. Chen
Institute of Biological Chemistry
Academia Sinica

E. coli 0.6 μm^3
1000 40 kDa proteins per second
15,000 ribosomes
1000*400/15000=27 a.a. per ribosome per second
1000 GroEL

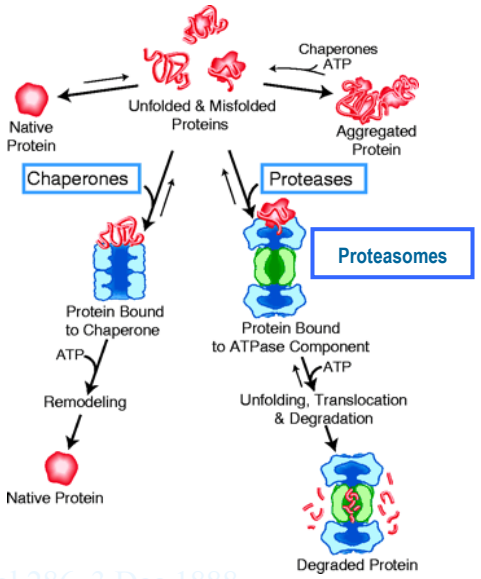

Science (1999) Vol 286 3 Dec 1888

Two families of molecular chaperone:

- DnaK/DnaJ/GrpE (or hsp70) family: bind to growing polypeptide chains while they are being synthesized by ribosomes and prevent premature folding (co-translational)
- Chaperonin family (GroE chaperonin): assist correct folding at a later stage (post-translational)

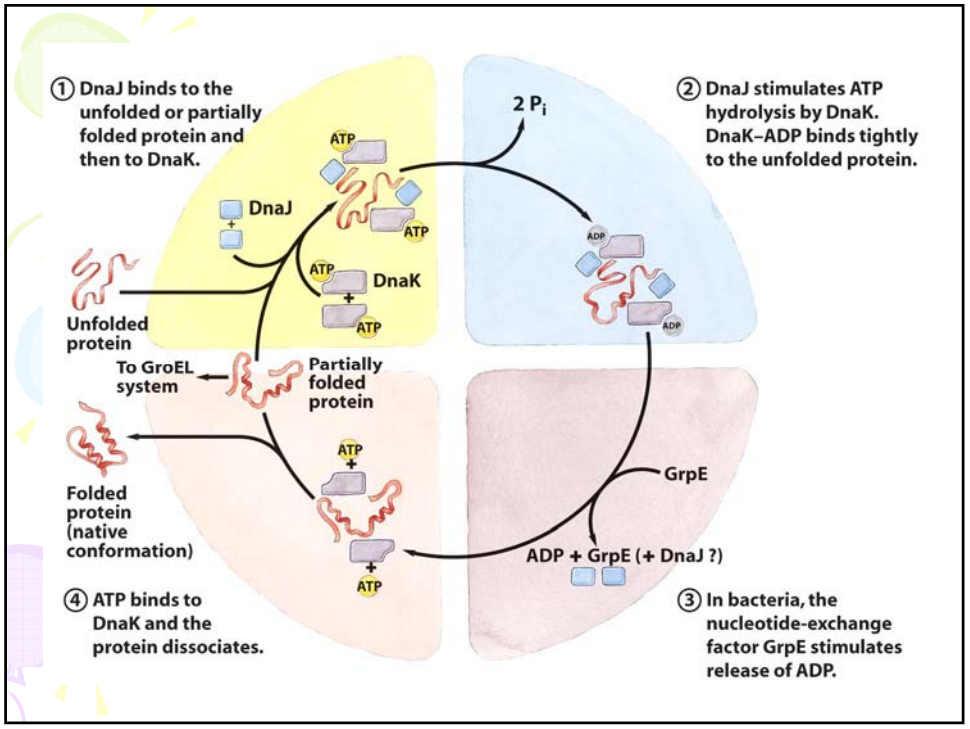

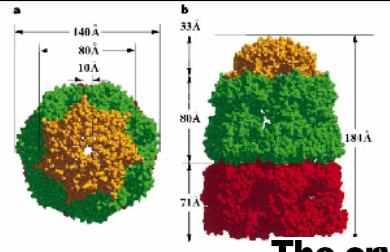

GroES: ;dome-shaped; heptameric ring of 10 kDa subunits

GroEL: cylindrical structure ;
two heptameric rings of ~57 kDa subunits

The crystal structure of the asymmetric GroEL–GroES–$(ADP)_7$ chaperonin complex

Zhaohui Xu*, Arthur L. Horwich† & Paul B. Sigler*

*The Howard Hughes Medical Institute, * The Department of Molecular Biophysics and Biochemistry, Yale University, 260 Whitney Avenue, and † The Department of Genetics, Yale University School of Medicine, Boyer Center for Molecular Medicine, 295 Congress Avenue, New Haven, Connecticut 06510, USA*

NATURE | VOL 388 | 21 AUGUST 1997

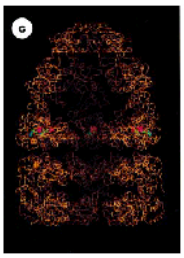

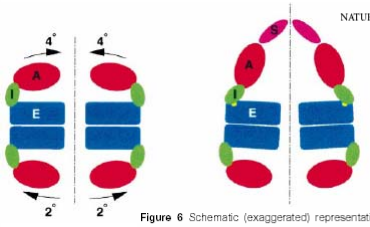

Figure 1 Overall architecture and dimensions of the GroEL–GroES complex. **a**, Van der Waals space-filling model of the entire complex in a top view looking down from the GroES-binding (*cis*) side; **b**, as **a**, but in a side view. The complex is colour coded as follows: *trans* GroEL ring, red; *cis* GroEL ring, green; GroES, gold. **c**, C_α drawing of the 'inside' of the GroEL–GroES complex. The view was produced by cutting the assembly open with a plane containing the 7-fold axis. ADP molecules bound to *cis* GroEL ring are shown as space-filling models. **a**, **b**, Produced using MidasPlus (Computer Graphics Laboratory, University of California, San Francisco); **c**, produced using program O[20].

Figure 6 Schematic (exaggerated) representation of the *en bloc* tilt of the equatorial domains and the subsequent deformation of the equatorial plane. E, equatorial domain; I, intermediate domain; A, apical domain; S, GroES subunit. The inward tilt in the *cis* ring is 4° and the complementary outward tilt in the *trans* ring is 2°. The interface between *cis* and *trans* rings is smooth and conserved in detail irrespective of the presence or absence of the *cis* assembly.

Chaperonin Function: Folding by Forced Unfolding

Mark Shtilerman,[1] George H. Lorimer,[2]* S. Walter Englander[1]

ATP and GroES binding

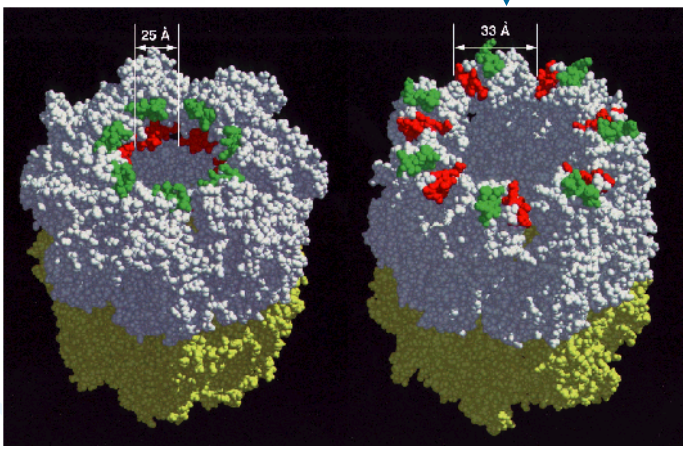

Fig. 1. (Top) The crystal structure of the asymmetric $GroEL_{14}$-$GroES_7$ complex solved by Xu *et al.* (*5*). The two opposed heptameric rings of GroEL are shown in white and yellow. The binding sites for GroES and the substrate protein are in the apical domains between each green and red helix pair (*3–5, 33*). In the less expanded ring (left), which captures the substrate protein, the binding sites are 25 Å from each other. On addition of ATP and GroES, the apical domain of each GroEL subunit twists upward and outward so that the binding sites move apart to a position 33 Å from one another, as shown in the open conformation at the right with the bound GroES removed for clarity. Neighboring binding sites move apart by 8 Å and non-neighboring sites by larger increments, up to 20 Å. A substrate protein tethered to these sites will be forcibly stretched and partially unfolded.

Functional cycle of chaperonins

Low affinity to nonnative protein in the presence of ATP

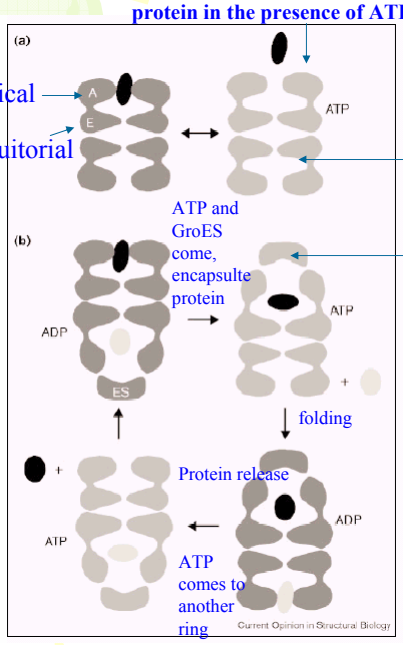

GroEL: cylindrical structure ;
two heptameric rings of ~57 kDa subunits

GroES: dome-shaped; heptameric ring of 10 kDa subunits

The functional cycle of chaperonins. (a) On the left is GroEL, with high affinity for non-native protein and, on the right, GroEL–ATP, with l affinity for non-native protein. ATPase activity sets up cycles of binding and release. A, apical domain; E, equatorial domain. (b) ATPase cy with GroEL, GroES (ES) and folding protein substrates. GroEL–GroES–ADP is the acceptor state for non-native protein. Subsequent ATP and GroES binding will encapsulate the protein. GroEL–GroES–ATP is the folding-active state. GroES binding alternates between rings and GroES release is stimulated by ATP binding to the opposite ring. Acceptor states are shown in dark gr and release states in light grey. The substrate is black and the second substrate in the full complex (b) is pale grey.

E. coli trigger factor

Ribosome-binding site

Peptidyl-prolyl isomerase

Co-translational folding

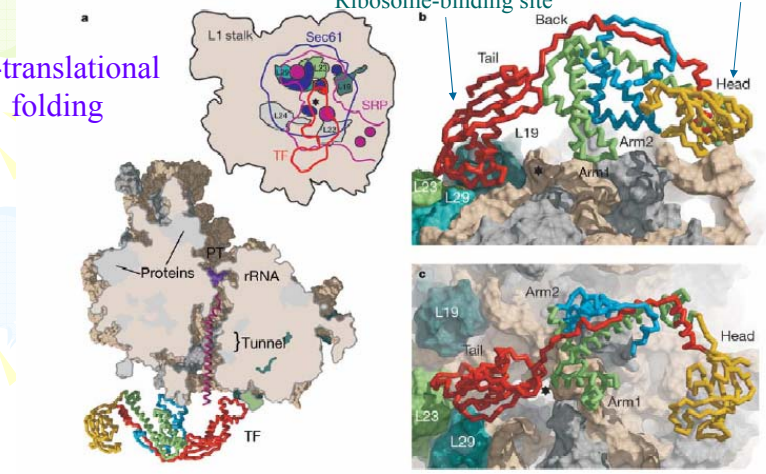

Figure 2 Structure of the trigger factor bound to the 50S ribosomal subunit. **a**, Overview of the trigger factor 50S complex. Full-length trigger factor positioned by superimposition onto the ribosome-bound fragment trigger factor 1–144 is shown as C_α-trace together with a slice of 50S along the peptide exit tunnel (for clarity, further cavities peripheral to the tunnel are not shown) with a modelled nascent chain in magenta, extending from the peptidyl transferase centre (PT). Colouring is as in Fig. 1. Inset: schematic footprints of Sec61, SRP and the trigger factor on the ribosome on the basis of crystallographic and electron microscopic data. Binding sites for Sec61p (blue), SRP (magenta) and the trigger factor (red) are represented as filled areas, and projections of the molecules are shown as outlines in the same colours. Positions of selected ribosomal proteins are indicated in the same colours as in Fig. 1. **b**, **c**, Close-up side (**b**) and top (**c**) views of the complex shown in **a** without a nascent peptide.

NATURE | VOL 431 | 30 SEPTEMBER 2004 | www.nature.com/nature

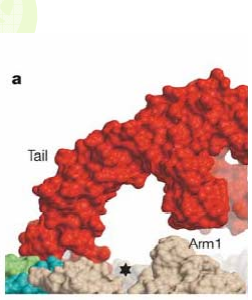

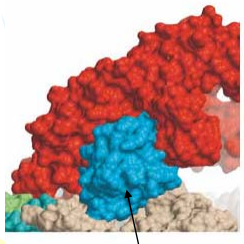

lysozyme

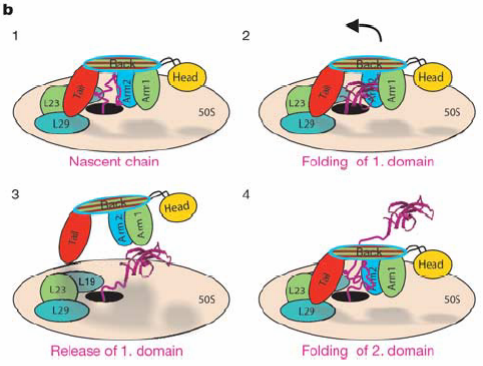

Figure 4 A model for the interaction of trigger factor with nascent chains. **a**, The trigger factor cradle could accommodate entire protein domains. Left: view through the arch-like structure delineated by the tail and arms of trigger factor (red) covering the peptide exit tunnel, indicated by an asterisk. Right: identical view to the lefthand figure; the size of the arch can accommodate an entire molecule of lysozyme (blue), manually fitted into this region for illustration. **b**, Schematic representation of the proposed mechanism of trigger factor action and its possible role in facilitating domain-wise co-translational protein folding. Colours are as in Fig. 2. Initially (1) the trigger factor is bound to an unfolded nascent chain. Upon folding of this domain (2), contacts between the trigger factor and the newly synthesized peptide are weakened and trigger factor dissociates from the ribosome (3). The trigger factor re-associates with the ribosome when the next stretch of newly synthesized, unfolded polypeptide becomes exposed (4).

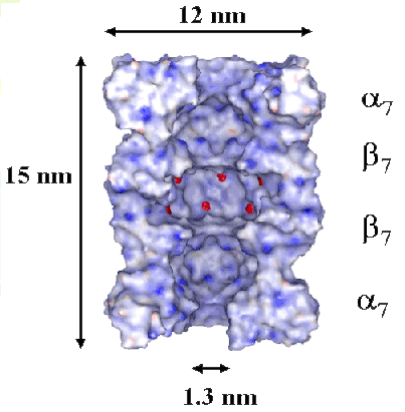

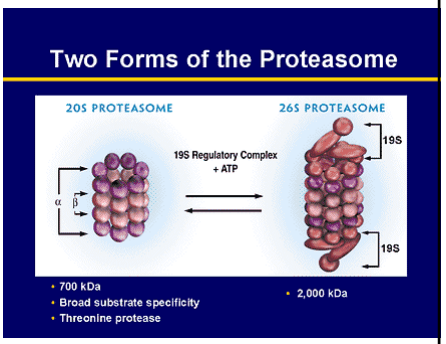

Predicted structure of the 20S proteasome from the methanoarchaeon *Methanosarcina thermophila*. The image is an atomic model based on the crystal structure coordinates of 20S proteasomes from *Thermoplasma acidophilum* and yeast. The active sites involved in peptide bond hydrolysis are indicated in red.

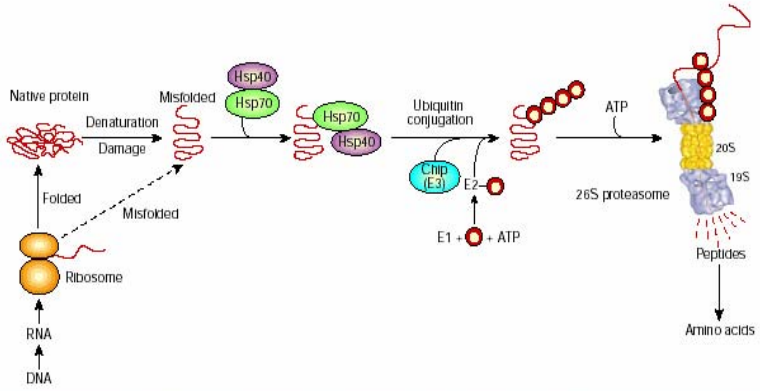

Figure 1 The ubiquitin–proteasome pathway. Molecular chaperones may function in protein folding and in the degradation of misfolded species. By associating with exposed hydrophobic domains, chaperones Hsp70/40 promote the folding of newly synthesized proteins and favours their refolding. Alternatively, they can facilitate the recognition of abnormal proteins, leading to their ubiquitylation by CHIP, the E3, and their degradation by the 26S proteasome. The red circles represent ubiquitin.

Protein degradation and protection against misfolded or damaged proteins

Alfred L. Goldberg

NATURE | VOL 426 | 18/25 DECEMBER 2003 p-895

Garrett & Grisham: Biochemistry, 2/e
Figure 1.17

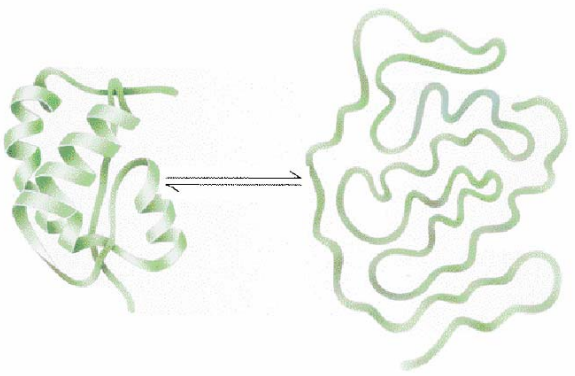

Nature

Denatured

Saunders College Publishing

First report of protein refolding *in vitro*

Anson and Mirsky

Alkali-denatured hemoglobin spontaneously recover its biological properties when the pH is returned to neutrality.

Anson, M.L. and Mirsky, A. E. (1925) J. Physiol. **60**, 50-67.

Renaturation of unfolded, denatured ribonuclease

Christian Anfinsen

C. Anfinsen, 1972 Nobel Laureate

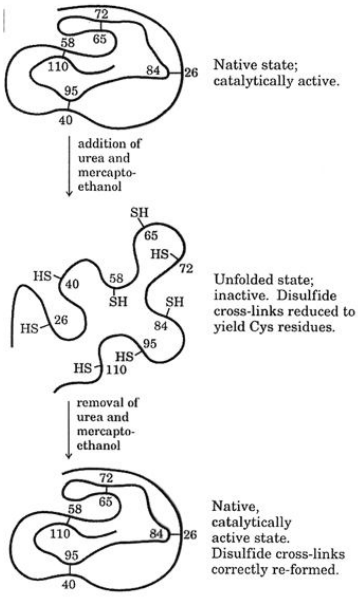

The amino acid sequence of a polypeptide chain contains all the information required to fold the chain into its native, 3D structure.

Anfinsen, C. B., Haber, E., Sela, M. and White, F. H. (1961) *Proc. Natl. Acad. Sci. USA* **47**, 1309-1314.

Structure and Mechanism in protein science
Alan Fersht

Table 17.3 *α-Helix- and β-sheet stabilizing effects of amino acids relative to alanine*[a]

Amino acid	Relative helix stability[a] (kcal/mol)	(kJ/mol)	Agadir[b] (kcal/mol)	(kJ/mol)	Relative β-sheet stability[c] (kcal/mol)	(kJ/mol)
Ala	0.00	0.0	0.00	0.00	0.00	0.00
Arg	0.17	0.7	0.06	0.25	−0.40	−1.7
Leu	0.17	0.7	0.19	0.79	−0.45	−1.9
Glu (0)[d]	0.17	0.7	—	—	—	—
Met	0.19	0.8	0.21	0.88	−0.90	−3.8
Lys	0.31	1.3	0.15	0.63	−0.35	−1.5
Trp	0.31	1.3	0.47	1.97	−1.04	−4.2
Gln	0.33	1.4	0.32	1.34	−0.38	−1.6
Ser	0.44	1.8	0.52	2.18	0.87	3.6
Ile	0.43	1.8	0.35	1.46	−1.25	−5.2
Phe	0.47	2.0	0.47	1.97	−1.08	−4.5
Cys	0.54	2.3	0.61	2.55	−0.78	−3.3
Asp (0)[d]	0.54	2.3	—	—	—	—
Glu (−)	0.56	2.3	0.34	1.42	−0.23	−1.0
Tyr	0.56	2.4	0.47	1.97	−1.63	−6.8
Asn	0.61	2.6	0.60	2.51	−0.52	−2.2
Thr	0.61	2.6	0.57	2.38	−1.36	−5.7
Val	0.63	2.7	0.51	2.13	−0.94	−3.9
His (0)	0.65	2.7	0.62	2.59	−0.37	−2.4
Asp (−)[d]	0.68	2.8	0.59	2.47	0.85	3.6
His (+)	0.88	3.7	—	—	—	—
Gly	0.90	3.8	1.11	4.64	1.21	5.1
Pro	3.47	14.5	2.72	11.4	>5	>20

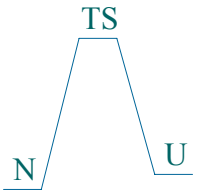

The transition from one conformation to another could be rapid or slow even if the two conformations are of comparable energy, depending on the heights of the barrier connecting the two conformational states in phase space

Unfolding temperature T_m:

$\Delta G(T) = \Delta H(T) - T_m \Delta S(T) \approx 0$, for $T \approx T_m$

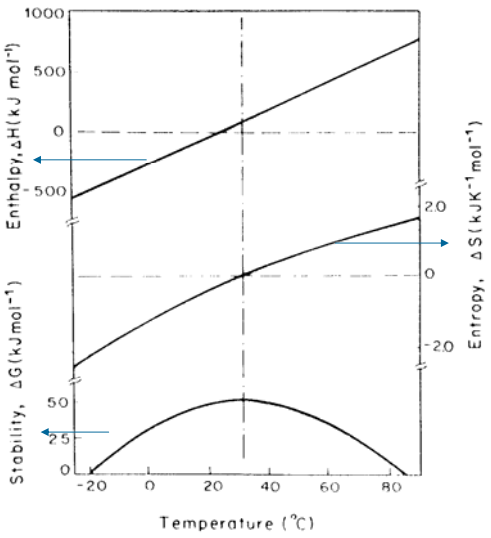

FIG. 12. The enthalpy, entropy, and Gibbs energy differences between native and denatured states of CN-metmyoglobin in 40 m*M* glycine solution, pH 10.7.

Protein folding theory

Protein with 100 amino acid residues

⇩

Assume 2 conformations for each residue

⇩

10^{30} possibilities

⇩

10^{7} years of random searching

Are there pathways for protein folding?

C. Levinthal, J. de Chim. Phys. **65**, 44 (1968).

Unfolded

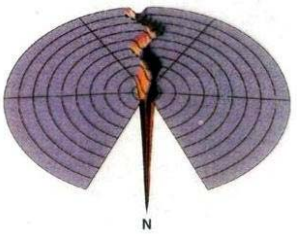

Native

K.A. Dill & H.S. Chan, *Nature Struct. Biol.* **4**, 4 (1997).

Levinthal Paradox:

How do proteins find the native "needle" in the conformational "haystack" in milliseconds when the free energy bias toward the native state is so small?

Folding models:

Framework model
Hydrophobic collapse mode
Nucleation condensation model
Funnel model
……

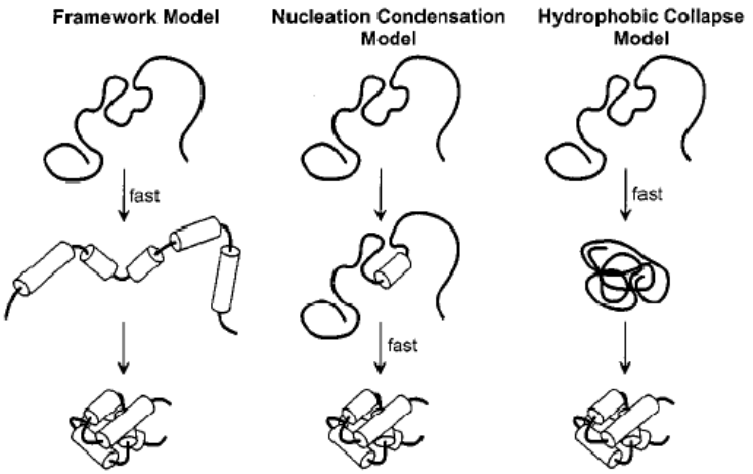

Protein Folding Funnel

Peter Leopold and Jose Onuchic introduced the protein folding funnel approach to the problem. (*PNAS 1992*)

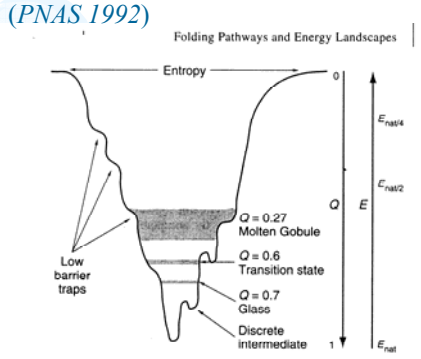

Figure 19.16 Cross section through a folding funnel. *E* corresponds to free energy. [Courtesy of P. G. Wolynes]

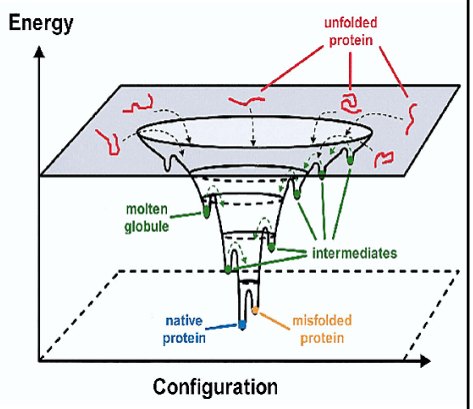

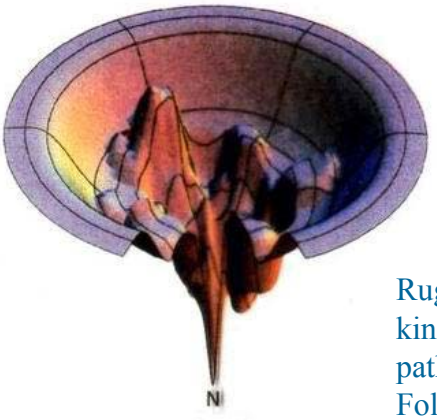

Rugged energy landscape with kinetic traps, energy barriers, pathways to the native state. Folding can be multi state

Fig. 1 The cartoon illustrates that a blind man develops a very wrong impression of an elephant depending on which body parts he touches, demonstrating the importance of the examination of a folding reaction by as many probes as possible prior to drawing conclusions.

Yeh & Rousseau (2000) Nature Structural Biology 7, 443-445.

Table 1. Methods used to investigate protein folding and aggregation

Property	Technique	Measurement
Chain packing	Intrinsic fluorescence	The orientation and environment of (predominantly) tryptophan side chains
	Ultraviolet absorbance	The orientation and environment of aromatic side chains
	Extrinsic (ANS) fluorescence	Formation and disruption of organized hydrophobic patches and clefts
	Fluorescence quenching	Isolation of tryptophan side chains from hydrophilic fluorescence quenchers
	Cysteinyl quenching	Protection of cysteine side chains from hydrophilic reactants
Molecular dimensions	Fluorescence anisotropy	Tryptophan side chain mobility and overall molecular dimensions
	Fluorescence energy transfer	Scalar distance between tryptophan and a covalently attached fluorophore (or between two attached fluorophores)
	Small angle X-ray scattering/Quasi-elastic light scattering	The average radius of gyration
	NMR diffusion measurements	The effective hydrodynamic radius

Continued

Secondary structure and persistent hydrogen bonds	Far-UV circular dichroism	Backbone conformation averaged over sequence and population
	Fourier transfer infra-red	Backbone conformation, hydrogen bond properties
	Pulse labelling NMR	Sequence specific formation of stable amide and tryptophan hydrogen bonds
	Pulse labelling mass spectrometry	The formation and cooperativity of persistent hydrogen bonds in discrete intermediates
Tertiary contacts and native structure	Biological activity	The formation of native tertiary structure at the active site
	Interrupted folding	The unfolding rate of discrete intermediates as a probe of their stability
	Near-UV circular dichroism	Formation of stable aromatic and disulphide bond tertiary contacts
	Real-time NMR	Formation of specific side chain tertiary contacts
	Protein engineering	The energetic contributions of side chains to discrete intermediates
	AFM/laser tweezers	Force required to unfold protein or region of protein
Aggregate structure	Congo red or thioflavin fluorescence	Existence of regular β-sheet structure
	Birefringence with Congo red	Well-defined amyloid core structure
	X-ay fibre diffraction	Spacings of regular elements of structure e.g. β-sheets
	AFM/EM	Dimensions and morphology of discrete aggregates
	Solid state NMR	Molecular conformation and intermolecular packing

Measuring protein stability…….

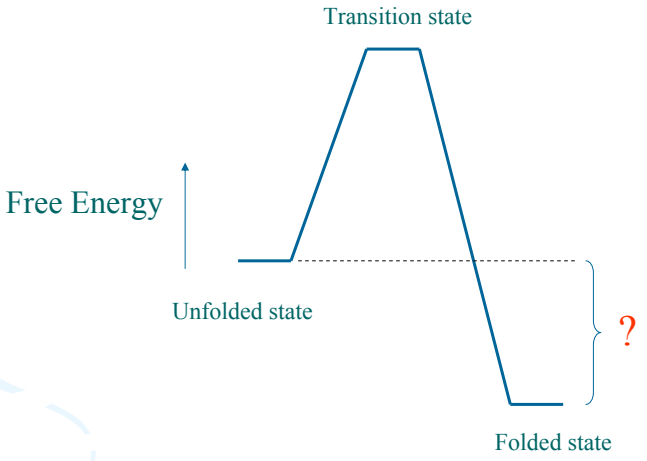

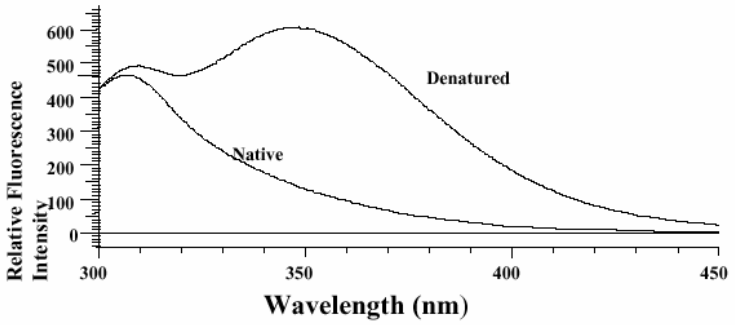

Figure 1: Urea-induced unfolding of nFGF-1 monitored by the changes in the intrinsic tryptophan fluorescence spectra of nFGF-1 in the native and unfolded states. The unfolded state of the protein is characterized by an enhanced fluorescence at 350 nm.

Two state model

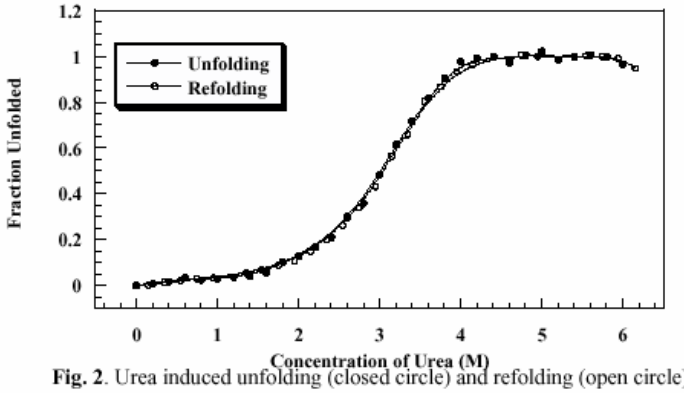

Fig. 2. Urea induced unfolding (closed circle) and refolding (open circle). This shows that the refolding is reversible

$$K_{fold} = \frac{f_F}{f_U} = \frac{f_F}{1-f_F} = \frac{y_U - y}{y - y_F}$$

$$\Delta G_{fold} = - RT \ln K_{fold}$$

$$\Delta G_{fold} = \Delta G^{H2O} - m[GdnHCl]$$

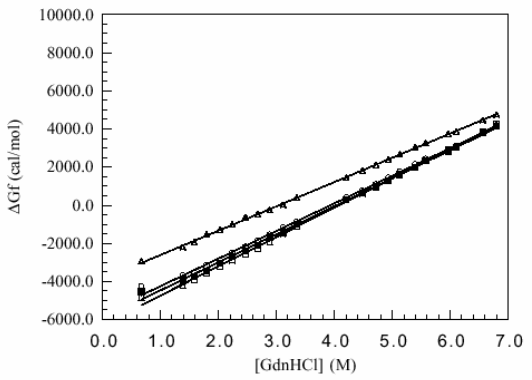

$$\Delta G_{fold} = - RT \ln K = -RT \ln(y_F/y_U) = 0$$

$$C_m = \Delta G^{H2O}/m$$

Measuring folding & unfolding rate…….

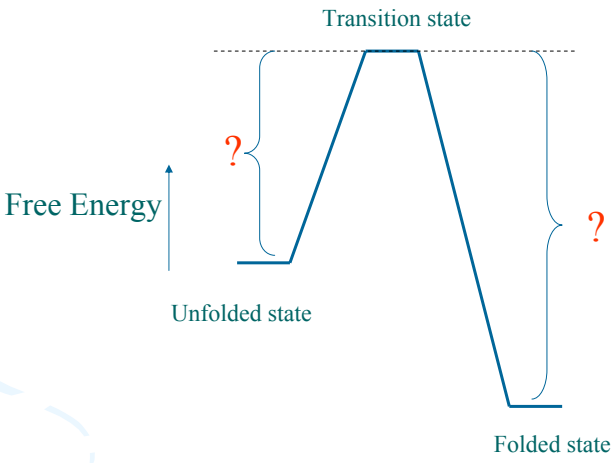

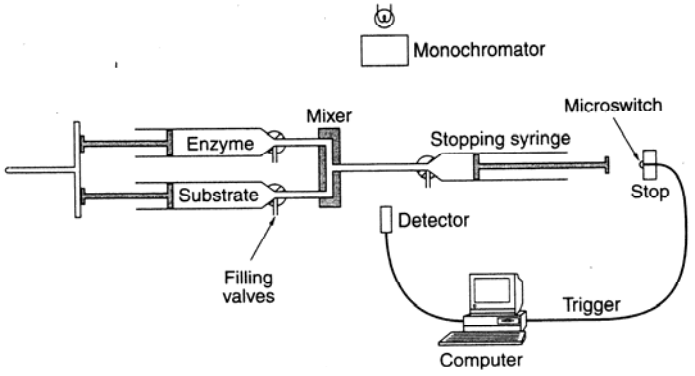

Figure 4.3 Stopped-flow apparatus.

Stopped Flow: how does it work?

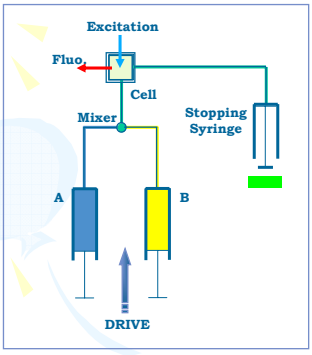

Standard stopped flow schematic

- Under pneumatic drive activation, the two small volumes of solutions are driven from high performance syringes through a high efficiency mixer.
- The resultant mixture passes through a measurement flow cell and into a stopping syringe.
- Just prior to stopping, a steady state flow is achieved.
- As the solution fills the stopping syringe, the plunger hits a block, causing the flow to be stopped instantaneously.
- Using appropriate techniques, the kinetics of the reaction can be measured in the cell.

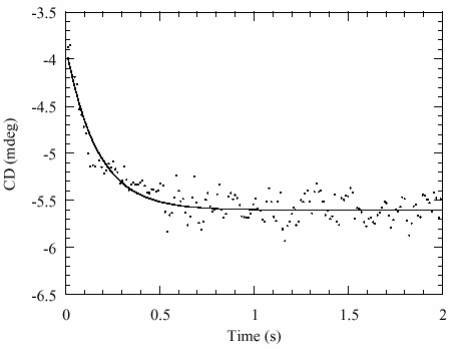

$A(t) = \Sigma A_i \exp(-k_i t) + A_\infty$

where A(t) is the amplitude of the change at time t, A_∞ is the amplitude at infinite time, A_i is the amplitude at zero time of phase i, and k_i is the rate of phase i.

Chevron plot

警員佩戴的山形(V形)臂章

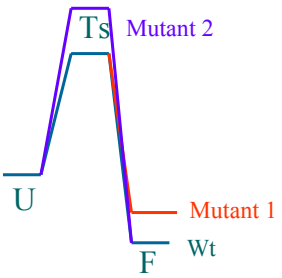

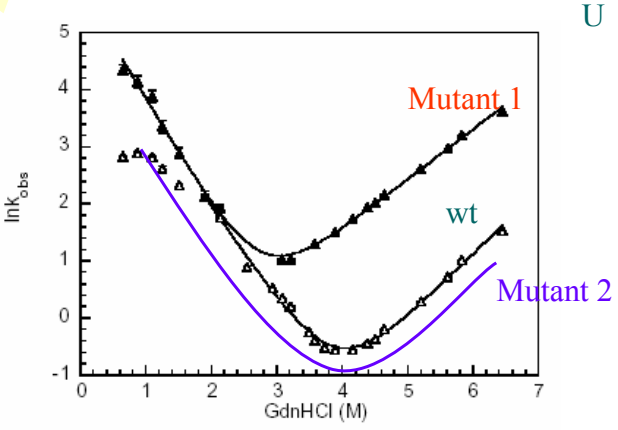

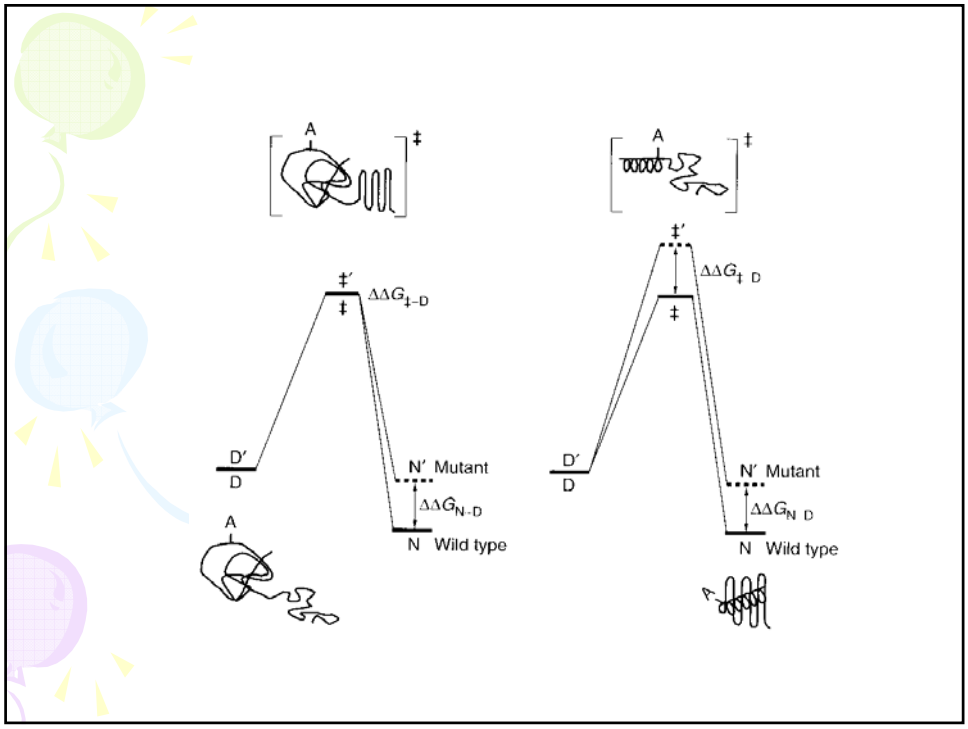

Stopped-flow fluorescence results in the refolding of cytochrome *c*

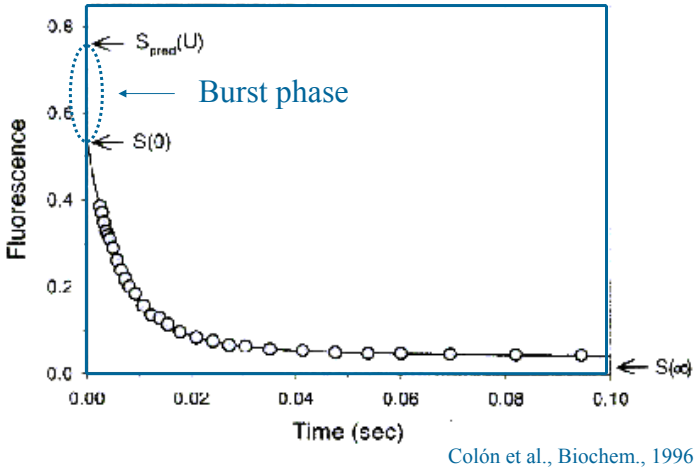

Colón et al., Biochem., 1996

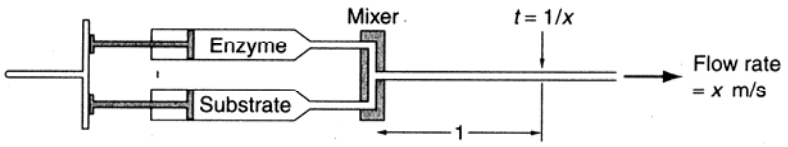

Figure 4.1 Continuous-flow apparatus.

For 1-cm window length, 10 m/s flow rate
observation time = 0.01/10 = 0.001 s = 1 ms

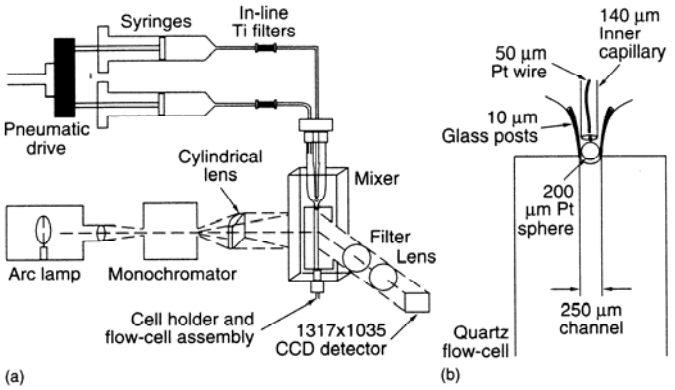

Figure 4.2 (a) Continuous-flow machine with 45-μs dead time. (b) Exploded view of the mixing chamber. Turbulent flow of the two liquids over the platinum sphere gives improved mixing. [Courtesy of M. C. Ramachrandra Shastry and H. Roder.]

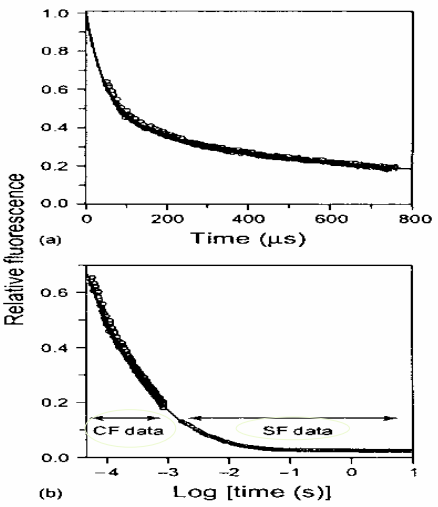

Figure 5 Example of protein folding kinetic measurement utilizing tryptophan fluorescence.[64] (a) Refolding of acid-unfolded horse cytochrome *c* was followed on the submillisecond timescale in a continuous flow capillary mixing apparatus. (b) Combination of continuous flow (CF) and conventional stopped-flow (SF) experiments allows collection of data over a wide range of time (symbols) and determination of the five kinetic phases with correlation times ranging from tens of microseconds to tens of milliseconds (solid line). (Reproduced by permission of the Biophysical Society.)

Hydrogen exchange

- Structural information from kinetic data

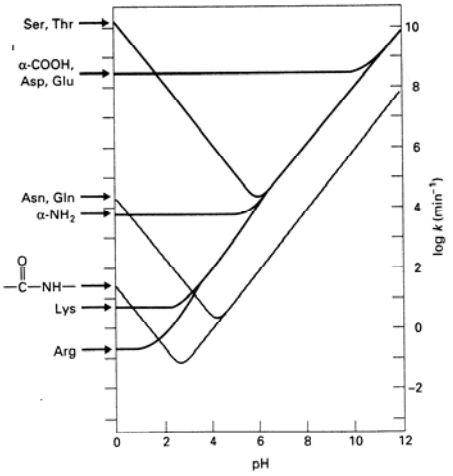

FIGURE 7.8
Dependence on pH of hydrogen exchange rates (k) of model groups.

When NH exchanges slower
It folds faster (and P higher)

P (Protection factor)
$= k_{int}/k_{ex}$

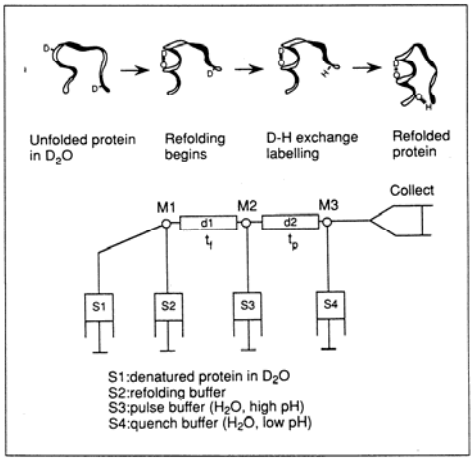

Fig. 1. Schematic illustration of the pulsed hydrogen exchange method. The basic principle is illustrated (*top*) with a hypothetical 'protein' with two representative amide probes. The first ND group becomes protected against exchange in a rapidly forming helical hydrogen bond and remains deuterated, while the second one is still exposed at this time and becomes protonated by D to H exchange during the labelling pulse. A diagram of a quenched-flow apparatus with three mixing stages (M1–M3) and two variable delay lines (d1 and d2) is shown (*below*). Syringes S1 and S2 are activated at t = 0 to initiate refolding by dilution of the denaturant in mixer M1. After a refolding time t_f, the protein solution is mixed in M2 with an H_2O buffer at basic pH (typically pH 9–10) to start the D to H exchange reaction. After a pulse time t_p, exchange is quenched by lowering the pH in M3 under conditions that favour rapid refolding.

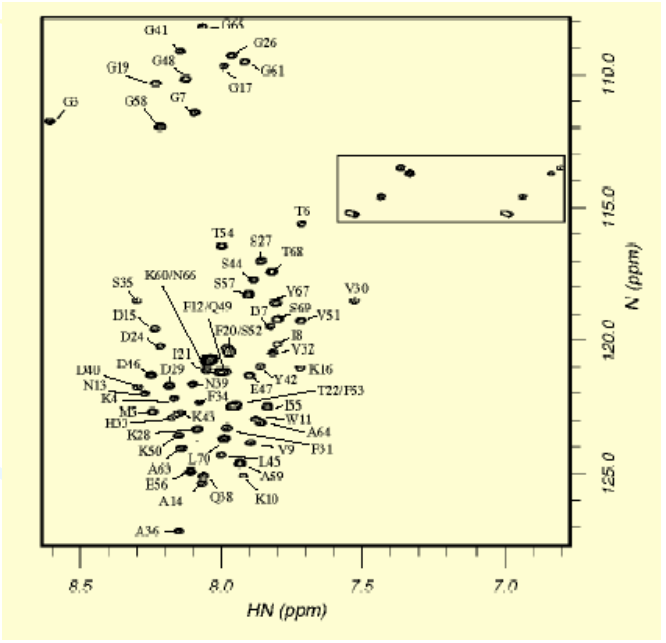

Timescales of experiments for studying protein folding

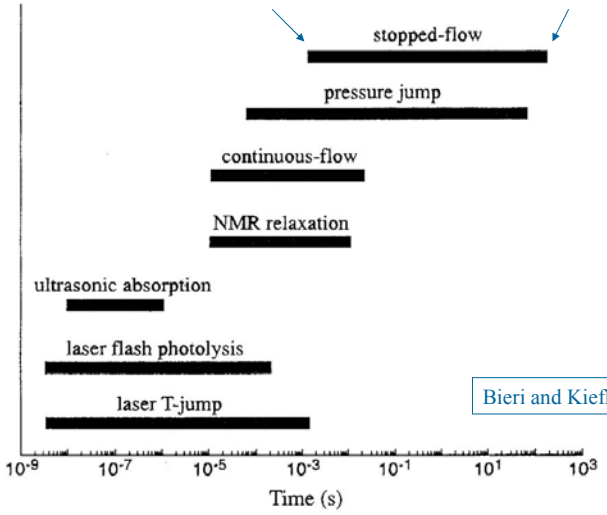

Bieri and Kiefhber, Biol. Chem., 1999

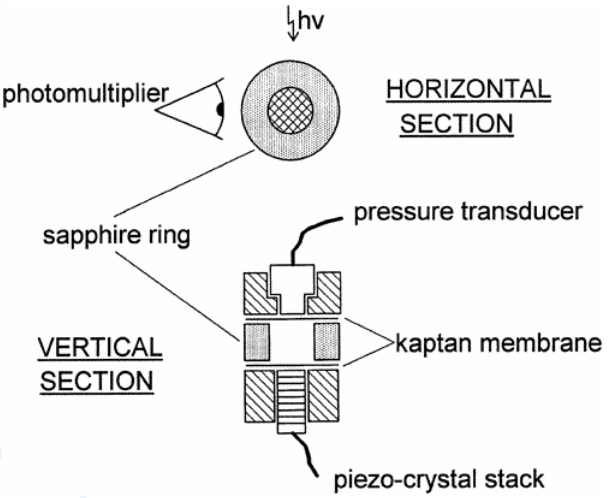

Schematic diagram of the pressure-jump apparatus

Jacob et al. Biochemistry 38, 2882-2891

Temperature jump

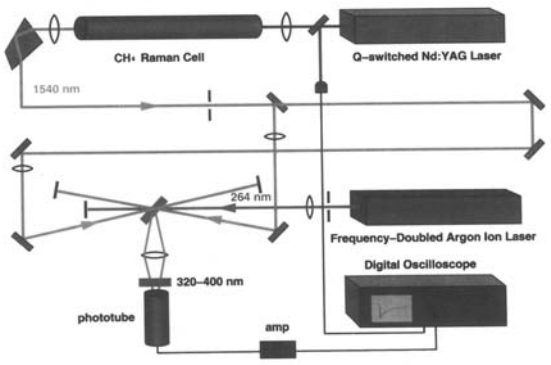

Fig. 4. Schematic of the temperature-jump instrument. An ~5 ns (FWHM) temperature-jump pulse is generated using the stimulated Raman effect to shift the Nd:YAG fundamental (1064 nm) to 1.54 μm in a mixture of CH_4 and He gas. 10 mJ of 1.54 μm light is split into two beams which are focused onto the 500 μm path-length sample cell to give a spot size of 0.5 mm. A cw UV beam at 264 nm from an intracavity-frequency-doubled argon ion laser is focused to a spot size of 60–70 μm to excite the tryptophan chromophore. The fluorescence signal is collected at 90° from the excitation beam, filtered using a bandpass filter, and measured using an end-window photomultiplier tube.

CO flash photolysis

- Reduced [Fe(Ⅱ)] cytochrome *c* is strongly destabilized in the presence of CO, which preferentially binds to the heme iron in the unfolded state. The photodissociation of CO by a short laser pulse initiates folding because the CO-free protein is much more stable at the same solvent condition

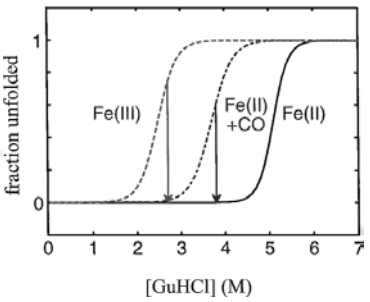

Photoreduction of the cytochrome *c* heme (rapid electron transfer)

- Pascher et al. studied the folding of cytochrome *c* by using various photoreductants to inject an electron into the heme of unfolded ferricytochrome *c* titrated with 2.3 to 4.6 M GuHCl at pH 7 and 40 ℃ to produce unfolded ferrocytochrome, which then converted to the folded protein